
Convolutional Normalizing Flows

Guoqing Zheng¹ Yiming Yang¹ Jaime Carbonell¹

Abstract

Bayesian posterior inference is prevalent in various machine learning problems. Variational inference provides one way to approximate the posterior distribution, however its expressive power is limited and so is the accuracy of resulting approximation. Recently, there has a trend of using neural networks to approximate the variational posterior distribution due to the flexibility of neural network architecture. One way to construct flexible variational distribution is to warp a simple density into a complex by normalizing flows, where the resulting density can be analytically evaluated. However, there is a trade-off between the flexibility of normalizing flow and computation cost for efficient transformation. In this paper, we propose a simple yet effective architecture of normalizing flows, *ConvFlow*, based on convolution over the dimensions of random input vector. Experiments on synthetic and real world posterior inference problems demonstrate the effectiveness and efficiency of the proposed method.

1. Introduction

Posterior inference is the key to Bayesian modeling, where we are interested to see how our belief over the variables of interest change after observing a set of data points. Predictions can also benefit from Bayesian modeling as every prediction will be equipped with confidence intervals representing how sure the prediction is. Compared to the maximum a posterior estimator of the model parameters, which is a point estimator, the posterior distribution provide richer information about the model parameter hence enabling more justified prediction.

Among the various inference algorithms for posterior estimation, variational inference (VI) and Monte Carlo Markov

chain (MCMC) are the most two widely used ones. It is well known that MCMC suffers from slow mixing time though asymptotically the samples from the chain will be distributed from the true posterior. VI, on the other hand, facilitates faster inference, since it is optimizing an explicit objective function and convergence can be measured and controlled, and it's been widely used in many Bayesian models, such as Latent Dirichlet Allocation (Blei et al., 2003), etc. However, one drawback of VI is that it makes strong assumption about the shape of the posterior such as the posterior can be decomposed into multiple independent factors. Though faster convergence can be achieved by parameter learning, the approximating accuracy is largely limited.

The above drawbacks stimulates the interest for richer function families to approximate posteriors while maintaining acceptable learning speed. Specifically, neural network is one among such models which has large modeling capacity and endows efficient learning. (Rezende & Mohamed, 2015) proposed normalization flow, where the neural network is set up to learn an invertible transformation from one known distribution, which is easy to sample from, to the true posterior. Model learning is achieved by minimizing the KL divergence between the empirical distribution of the generated samples and the true posterior. After properly trained, the model will generate samples which are close to the true posterior, so that Bayesian predictions are made possible. Other methods based on modeling random variable transformation, but based on different formulations are also explored, including NICE (Dinh et al., 2014), the Inverse Autoregressive Flow (Kingma et al., 2016), and Real NVP (Dinh et al., 2016).

One key component for normalizing flow to work is to compute the determinant of the Jacobian of the transformation, and in order to maintain fast Jacobian computation, either very simple function is used as the transformation, such as the planar flow in (Rezende & Mohamed, 2015), or complex tweaking of the transformation layer is required. Alternatively, in this paper we propose a simple and yet effective architecture of normalizing flows, based on convolution on the random input vector. Due to the nature of convolution, bi-jjective mapping between the input and output vectors can be easily established; meanwhile, efficient computation of the determinant of the convolution Jacobian is achieved linearly. We further propose to incorporate dilated convo-

¹School of Computer Science, Carnegie Mellon University, Pittsburgh PA, USA. Correspondence to: Guoqing Zheng <gzheng@cs.cmu.edu>.

lution (Yu & Koltun, 2015; Oord et al., 2016a) to model long range interactions among the input dimensions. The resulting convolutional normalizing flow, which we term as *Convolutional Flow (ConvFlow)*, is simple and yet effective in warping simple densities to match complex ones.

The remainder of this paper is organized as follows: We briefly review the principles for normalizing flows in Section 2, and then present our proposed normalizing flow architecture based on convolution in Section 3. Empirical evaluations and analysis on both synthetic and real world data sets are carried out in Section 4, and we conclude this paper in Section 5.

2. Preliminaries

2.1. Transformation of random variables

Given a random variable $z \in \mathbb{R}^d$ with density $p(z)$, consider a smooth and invertible function $f : \mathbb{R}^d \rightarrow \mathbb{R}^d$ operated on z . Let $z' = f(z)$ be the resulting random variable, the density of z' can be evaluated as

$$p(z') = p(z) \left| \det \frac{\partial f^{-1}}{\partial z'} \right| = p(z) \left| \det \frac{\partial f}{\partial z} \right|^{-1} \quad (1)$$

thus

$$\log p(z') = \log p(z) - \log \left| \det \frac{\partial f}{\partial z} \right| \quad (2)$$

2.2. Normalizing flows

Normalizing flows considers successively transforming z_0 with a series of transformations $\{f_1, f_2, \dots, f_K\}$ to construct arbitrarily complex densities for $z_K = f_K \circ f_{K-1} \circ \dots \circ f_1(z_0)$ as

$$\log p(z_K) = \log p(z_0) - \sum_{k=1}^K \log \left| \det \frac{\partial f_k}{\partial z_{k-1}} \right| \quad (3)$$

Hence the complexity lies in computing the determinant of the Jacobian matrix. Without further assumption about f , the general complexity for that is $\mathcal{O}(d^3)$ where d is the dimension of z . In order to accelerate this, (Rezende & Mohamed, 2015) proposed the following family of transformations that they termed as *planar flow*:

$$f(z) = z + \mathbf{u}h(\mathbf{w}^\top z + b) \quad (4)$$

where $\mathbf{w} \in \mathbb{R}^d$, $\mathbf{u} \in \mathbb{R}^d$, $b \in \mathbb{R}$ are parameters and $h(\cdot)$ is a univariate non-linear function with derivative $h'(\cdot)$. For this family of transformations, the determinant of the Jacobian matrix can be computed as

$$\det \frac{\partial f}{\partial z} = \det(\mathbf{I} + \mathbf{u}\psi(z)^\top) = 1 + \mathbf{u}^\top \psi(z) \quad (5)$$

where $\psi(z) = h'(\mathbf{w}^\top z + b)\mathbf{w}$. The computation cost of the determinant is hence reduced from $\mathcal{O}(d^3)$ to $\mathcal{O}(d)$.

Applying f to z can be viewed as feeding the input variable z to a neural network with only one single hidden unit followed by a linear output layer which has the same dimension with the input layer. Obviously, because of the bottleneck caused by the single hidden unit, the capacity of the family of transformed density is hence limited.

3. A new transformation unit

In this section, we first propose a general extension to the above mentioned planar normalizing flow, and then propose a restricted version of that, which actually turns out to be convolution over the dimensions of the input random vector.

3.1. Normalizing flow with d hidden units

Instead of having a single hidden unit as suggested in planar flow, consider d hidden units in the process. We denote the weights associated with the edges from the input layer to the output layer as $\mathbf{W} \in \mathbb{R}^{d \times d}$ and the vector to adjust the magnitude of each dimension of the hidden layer activation as \mathbf{u} , and the transformation is defined as

$$f(z) = \mathbf{u} \odot h(\mathbf{W}z + b) \quad (6)$$

where \odot denotes the point-wise multiplication. The Jacobian matrix of this transformation is

$$\frac{\partial f}{\partial z} = \text{diag}(\mathbf{u} \odot h'(\mathbf{W}z + b))\mathbf{W} \quad (7)$$

$$\det \frac{\partial f}{\partial z} = \det[\text{diag}(\mathbf{u} \odot h'(\mathbf{W}z + b))] \det(\mathbf{W}) \quad (8)$$

As $\det(\text{diag}(\mathbf{u} \odot h'(\mathbf{W}z + b)))$ is linear, the complexity of computing the above transformation lies in computing $\det(\mathbf{W})$. Essentially the planar flow is restricting \mathbf{W} to be a vector of length d instead of matrices, however we can relax that assumption while still maintaining linear complexity of the determinant computation based on a very simple fact that the determinant of a triangle matrix is also just the product of the elements on the diagonal.

3.2. Convolutional Flow

Since normalizing flow with a fully connected layer may not be bijective and generally requires $\mathcal{O}(d^3)$ computations for the determinant of the Jacobian even it is, we propose to use 1-d convolution to transform random vectors.

Figure 1(a) illustrates how 1-d convolution is performed over an input vector and outputs another vector. We propose to perform a 1-d convolution on an input random vector z , followed by a non-linearity and necessary post operation

additional computation cost for the Jacobian as follows

$$z \rightarrow \underbrace{\text{ConvBlock} \rightarrow \text{Revert} \rightarrow \text{ConvBlock} \rightarrow \text{Revert} \rightarrow \dots \rightarrow f(z)}_{\text{Repetitions of ConvBlock+Revert for } K \text{ times}} \quad (13)$$

3.3. Connection to Inverse Autoregressive Flow

Inspired by the idea of constructing complex tractable densities from simpler ones with bijective transformations, different variants of the original normalizing flow (NF) (Rezende & Mohamed, 2015) have been proposed. Perhaps the one most related to ConvFlow is Inverse Autoregressive Flow (Kingma et al., 2016), which employs autoregressive transformations over the input dimensions to construct output densities. Specifically, one layer of IAF works as follows

$$f(z) = \mu(z) + \sigma(z) \odot z \quad (14)$$

where

$$[\mu(z), \sigma(z)] \leftarrow \text{AutoregressiveNN}(z) \quad (15)$$

are outputs from an autoregressive neural network over the dimensions of z . There are two drawbacks of IAF compared to the proposed ConvFlow:

- The autoregressive neural network over input dimensions in IAF is represented by a Masked Autoencoder (Germain et al., 2015), which generally requires $\mathcal{O}(d^2)$ parameters per layer, where d is the input dimension, while each layer of ConvFlow is much more parameter efficient, only needing $k + d$ parameters (k is the kernel size of 1d convolution and $k < d$).
- More importantly, due to the coupling of $\sigma(z)$ and z in the IAF transformation, in order to make the computation of the overall Jacobian determinant $\det \frac{\partial f}{\partial z}$ linear in d , the Jacobian of the autoregressive NN transformation is assumed to be *strictly* triangular (Equivalently, the Jacobian determinants of μ and σ w.r.t z are both always 0. This is achieved by letting the i th dimension of μ and σ depend only on dimensions $1, 2, \dots, i - 1$ of z). In other words, *the mappings from z onto $\mu(z)$ and $\sigma(z)$ via the autoregressive NN are always singular, no matter how their parameters are updated, and because of this, μ and σ will only be able to cover a subspace of the input space z belongs to*, which is obviously less desirable for a normalizing flow.² Though

²Since the singular transformations will only lead to subspace coverage of the resulting variable μ and σ , one could try to alleviate the subspace issue by modifying IAF to set both μ and σ as free parameters to be learned, the resulting normalizing flow of which is exactly a version of planar flow as proposed in (Rezende & Mohamed, 2015).

these singularity transforms in the autoregressive NN are somewhat mitigated by their final coupling with the input z , IAF still performs slightly worse in empirical evaluations than ConvFlow as no singular transform is involved in ConvFlow.

- Lastly, despite the similar nature of modeling variable dimension with an autoregressive manner, ConvFlow is much more efficient since the computation of the flow weights w and the input z is carried out by fast native 1-d convolutions, where IAF in its simplest form needs to maintain a masked feed forward network (if not maintaining an RNN). Similar idea of using convolution operators for efficient modeling of data dimensions is also adopted by PixelCNN (Oord et al., 2016b).

4. Experiments

We test performance the proposed ConvFlow on two settings, one on synthetic data to infer unnormalized target density and the other on density estimation for hand written digits and characters.

4.1. Synthetic data

We conduct experiments on using the proposed ConvFlow to approximate an unnormalized target density of z with dimension 2 such that $p(z) \propto \exp(-U(z))$. We adopt the same set of energy functions $U(z)$ in (Rezende & Mohamed, 2015) for a fair comparison, which is reproduced below

$$U_1(z) = \frac{1}{2} \left(\frac{\|z\| - 2}{4} \right)^2 - \log \left(e^{-\frac{1}{2} \left[\frac{z_1 - 2}{0.6} \right]^2} + e^{-\frac{1}{2} \left[\frac{z_1 + 2}{0.6} \right]^2} \right)$$

$$U_2(z) = \frac{1}{2} \left[\frac{z_2 - w_1(z)}{0.4} \right]^2$$

where $w_1(z) = \sin\left(\frac{\pi z_1}{2}\right) r$. The target density of z are plotted as the left most column in Figure 2, and we test to see if the proposed ConvFlow can transform a two dimensional standard Gaussian to the target density by minimizing the KL divergence

$$\begin{aligned} KL(q_K(z_k) || p(z)) &= \mathbb{E}_{z_k} \log q_K(z_k) - \mathbb{E}_{z_k} \log p(z_k) \\ &= \mathbb{E}_{z_0} \log q_0(z_0) - \mathbb{E}_{z_0} \log \left| \det \frac{\partial f}{\partial z_0} \right| + \mathbb{E}_{z_0} U(f(z_0)) + \text{const} \end{aligned} \quad (16)$$

where all expectations are evaluated with samples taken from $q_0(z_0)$. We use a 2-d standard Gaussian as $q_0(z_0)$ and we test different number of ConvBlocks stacked together in this task. Each ConvBlock in this case consists a ConvFlow layer with kernel size 2, dilation 1 and followed by another ConvFlow layer with kernel size 2, dilation 2. Revert Layer is appended after each ConvBlock, and tanh activation function is adopted by ConvFlow. The Autoregressive NN in

IAF is implemented as a two layer masked fully connected neural network (Germain et al., 2015).

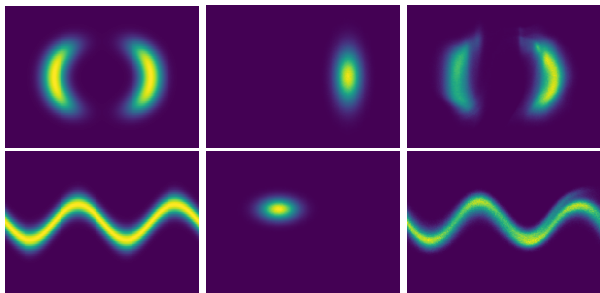


Figure 2: (a) True density; (b) Density learned by IAF (16 layers); (c) Density learned by ConvFlow. (8 blocks with each block consisting of 2 layers)

Experimental results are shown in Figure 2 for IAF (middle column) and ConvFlow (right column) to approximate the target density (left column). Even with 16 layers, IAF puts most of the density to one mode, confirming our analysis about the singular transform problem in IAF: As the data dimension is only two, the subspace modeled by $\mu(z)$ and $\sigma(z)$ in Eq. (14) will be lying on a 1-d space, i.e., a straight line, which is shown in the middle column. The effect of singular transform on IAF will be less severe for higher dimensions. While with 8 layers of ConvBlocks (each block consists of 2 1d convolution layers), ConvFlow is already approximating the target density quite well despite the minor underestimate about the density around the boundaries.

4.2. Handwritten digits and characters

4.2.1. SETUPS

To test the proposed ConvFlow for variational inference we use standard benchmark datasets MNIST³ and OMNIGLOT⁴ (Lake et al., 2013). Our method is general and can be applied to any formulation of the generative model $p_\theta(x, z)$; For simplicity and fair comparison, in this paper, we focus on densities defined by stochastic neural networks, i.e., a broad family of flexible probabilistic generative models with its parameters defined by neural networks. Specifically, we consider the following two family of generative models

$$G_1 : p_\theta(x, z) = p_\theta(z)p_\theta(x|z) \quad (17)$$

$$G_2 : p_\theta(x, z_1, z_2) = p_\theta(z_1)p_\theta(z_2|z_1)p_\theta(x|z_2) \quad (18)$$

³Data downloaded from http://www.cs.toronto.edu/~larocheh/public/datasets/binarized_mnist/

⁴Data downloaded from <https://github.com/yburda/iwae/raw/master/datasets/OMNIGLOT/chardata.mat>

where $p(z)$ and $p(z_1)$ are the priors defined over z and z_1 for G_1 and G_2 , respectively. All other conditional densities are specified with their parameters θ defined by neural networks, therefore ending up with two stochastic neural networks. This network could have any number of layers, however in this paper, we focus on the ones which only have one and two stochastic layers, i.e., G_1 and G_2 , to conduct a fair comparison with previous methods on similar network architectures, such as VAE, IWAE and Normalizing Flows.

We use the same network architectures for both G_1 and G_2 as in (Burda et al., 2015), specifically shown as follows

G_1 : A single Gaussian stochastic layer z with 50 units. In between the latent variable z and observation x there are two deterministic layers, each with 200 units;

G_2 : Two Gaussian stochastic layers z_1 and z_2 with 50 and 100 units, respectively. Two deterministic layers with 200 units connect the observation x and latent variable z_2 , and two deterministic layers with 100 units are in between z_2 and z_1 .

where a Gaussian stochastic layer consists of two fully connected linear layers, with one outputting the mean and the other outputting the logarithm of diagonal covariance. All other deterministic layers are fully connected with tanh non-linearity. Bernoulli observation models are assumed for both MNIST and OMNIGLOT. For MNIST, we employ the static binarization strategy as in (Larochelle & Murray, 2011) while dynamic binarization is employed for OMNIGLOT.

The inference networks $q(z|x)$ for G_1 and G_2 have similar architectures to the generative models, with details in (Burda et al., 2015). ConvFlow is hence used to warp the output of the inference network $q(z|x)$, assumed to be Gaussian conditioned on the input x , to match complex true posteriors. Our baseline models include VAE (Kingma & Welling, 2013), IWAE (Burda et al., 2015) and Normalizing Flows (Rezende & Mohamed, 2015). Since our proposed method involves adding more layers to the inference network, we also include another enhanced version of VAE with more deterministic layers added to its inference network, which we term as VAE+.⁵ With the same VAE architectures, we also test the abilities of constructing complex variational posteriors with IAF and ConvFlow, respectively. All models are implemented in PyTorch. Parameters of both the variational distribution and the generative distribution of all models are optimized with Adam (Kingma & Ba, 2014) for 2000 epochs, with a fixed learning rate of 0.0005, exponential decay rates for the 1st and 2nd moments at 0.9 and 0.999, respectively. Batch normalization (Ioffe & Szegedy, 2015)

⁵VAE+ adds more layers before the stochastic layer of the inference network while the proposed method is add convolutional flow layers after the stochastic layer.

and linear annealing of the KL divergence term between the variational posterior and the prior is employed for the first 200 epochs, as it has been shown to help training multi-layer stochastic neural networks (Sønderby et al., 2016). Code to reproduce all reported results will be made publicly available.

For inference models with latent variable z of 50 dimensions, a ConvBlock consists of following ConvFlow layers

$$\begin{aligned} & [\text{ConvFlow}(\text{kernel size} = 5, \text{dilation} = 1), \\ & \text{ConvFlow}(\text{kernel size} = 5, \text{dilation} = 2), \\ & \text{ConvFlow}(\text{kernel size} = 5, \text{dilation} = 4), \\ & \text{ConvFlow}(\text{kernel size} = 5, \text{dilation} = 8), \\ & \text{ConvFlow}(\text{kernel size} = 5, \text{dilation} = 16), \\ & \text{ConvFlow}(\text{kernel size} = 5, \text{dilation} = 32)] \quad (19) \end{aligned}$$

and for inference models with latent variable z of 100 dimensions, a ConvBlock consists of following ConvFlow layers

$$\begin{aligned} & [\text{ConvFlow}(\text{kernel size} = 5, \text{dilation} = 1), \\ & \text{ConvFlow}(\text{kernel size} = 5, \text{dilation} = 2), \\ & \text{ConvFlow}(\text{kernel size} = 5, \text{dilation} = 4), \\ & \text{ConvFlow}(\text{kernel size} = 5, \text{dilation} = 8), \\ & \text{ConvFlow}(\text{kernel size} = 5, \text{dilation} = 16), \\ & \text{ConvFlow}(\text{kernel size} = 5, \text{dilation} = 32), \\ & \text{ConvFlow}(\text{kernel size} = 5, \text{dilation} = 64)] \quad (20) \end{aligned}$$

A Revert layer is appended after each ConvBlock and leaky ReLU with a negative slope of 0.01 is used as the activation function in ConvFlow. For IAF, the autoregressive neural network is implemented as a two layer masked fully connected neural network.

4.2.2. GENERATIVE DENSITY ESTIMATION

For MNIST, models are trained and tuned on the 60,000 training and validation images, and estimated log-likelihood on the test set with 128 importance weighted samples are reported. Table 1 presents the performance of all models, when the generative model is assumed to be from both G_1 and G_2 .

Firstly, VAE+ achieves higher log-likelihood estimates than vanilla VAE due to the added more layers in the inference network, implying that a better posterior approximation is learned (which is still assumed to be a Gaussian). Second, we observe that VAE with ConvFlow achieves much better density estimates than VAE+, which confirms our expectation that warping the variational distribution with convolutional flows enforces the resulting variational posterior to match the true non-Gaussian posterior. Also, adding more blocks of convolutional flows to the network makes the

variational posterior further close to the true posterior. We also observe that VAE with Inverse Autoregressive Flows (VAE+IAF) improves over VAE and VAE+, due to its modeling of complex densities, however the improvements are not as significant as ConvFlow. The limited improvement might be explained by our analysis on the singular transformation and subspace issue in IAF. Lastly, combining convolutional normalizing flows with multiple importance weighted samples, as shown in last row of Table 1, further improvement on the test set log-likelihood is achieved. Overall, the method combining ConvFlow and importance weighted samples achieves best NLL on both settings, outperforming IWAE significantly by 7.1 nats on G_1 and 5.7 nats on G_2 . Notice that, ConvFlow combined with IWAE achieves an NLL of 79.11, comparable to the best published result of 79.10, achieved by PixelRNN (Oord et al., 2016b) with a much more sophisticated architecture. Also it’s about 0.8 nat better than the best IAF result of 79.88 reported in (Kingma et al., 2016), which demonstrates the representative power of ConvFlow compared to IAF⁶.

Results on OMNIGLOT are presented in Table 2 where similar trends can be observed as on MNIST. One observation different from MNIST is that, the gain from IWAE+ConvFlow over IWAE is not as large as it is on MNIST, which could be explained by the fact that OMNIGLOT is a more difficult set compared to MNIST, as there are 1600 different types of symbols in the dataset with roughly 20 samples per type. Again on OMNIGLOT we observe IAF with VAE improves over VAE and VAE+, while doesn’t perform as well as ConvFlow.

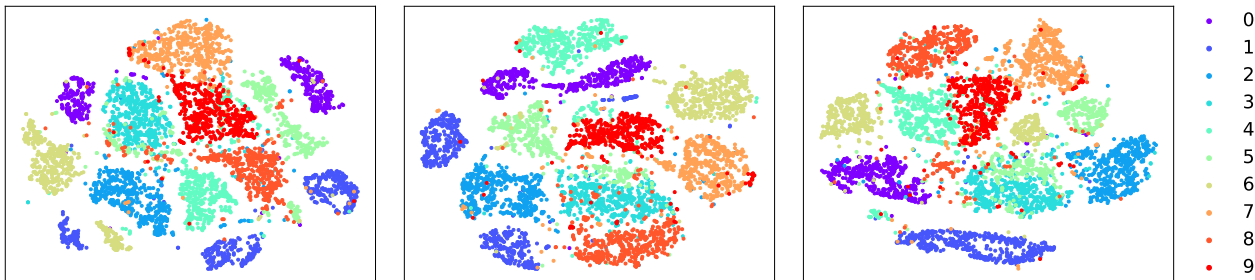
4.2.3. LATENT CODE VISUALIZATION

We visualize the inferred latent codes z of 5000 digits in the MNIST test set with respect to their true class labels in Figure 3 from different models with tSNE (Maaten & Hinton, 2008). We observe that on generative model G_2 , all three models are able to infer latent codes of the digits consistent with their true classes. However, VAE and VAE+IAF both show disconnected cluster of latent codes from the same class (e.g., digits 0 and digits 1). Latent codes inferred by VAE for digit 3 and 5 tend to mix with each other. Overall, VAE equipped with ConvFlow produces clear separable latent codes for different classes while also maintaining high in-class density (notably for digit classes 0, 1, 2, 7, 8, 9 as

⁶The result in (Kingma et al., 2016) are not directly comparable, as their results are achieved with a much more sophisticated VAE architecture and a much higher dimension of latent code ($d = 1920$ for the best NLL of 79.88). However, in this paper, we only assume a relatively simple VAE architecture compose of fully connected layers and the dimension of latent codes to be relatively low, 50 or 100, depending on the generative model in VAE. One could expect the performance of ConvFlow to improve even further if similar complex VAE architecture and higher dimension of latent codes are used.

Table 1: MNIST test set NLL with generative models G_1 and G_2 (lower is better K is number of ConvBlocks)

MNIST (static binarization)	$-\log p(x)$ on G_1	$-\log p(x)$ on G_2
VAE (Burda et al., 2015)	88.37	85.66
IWAE ($IW = 50$) (Burda et al., 2015)	86.90	84.26
VAE+NF (Rezende & Mohamed, 2015)	-	≤ 85.10
VAE+ ($K = 1$)	88.20	85.41
VAE+ ($K = 4$)	88.08	85.26
VAE+ ($K = 8$)	87.98	85.16
VAE+IAF ($K = 1$)	87.70	85.03
VAE+IAF ($K = 2$)	87.30	84.74
VAE+IAF ($K = 4$)	87.02	84.55
VAE+IAF ($K = 8$)	86.62	84.26
VAE+ConvFlow ($K = 1$)	86.91	85.45
VAE+ConvFlow ($K = 2$)	86.40	85.37
VAE+ConvFlow ($K = 4$)	84.78	81.64
VAE+ConvFlow ($K = 8$)	83.89	81.21
IWAE+ConvFlow ($K = 8, IW = 50$)	79.78	79.11

Figure 3: **Left:** VAE, **Middle:** VAE+IAF, **Right:**VAE+ConvFlow. (best viewed in color)

shown in the rightmost figure).

4.2.4. GENERATION

After the models are trained, generative samples can be obtained by feeding $z \sim N(0, I)$ to the learned generative model G_1 (or $z_2 \sim N(0, I)$ to G_2). Since higher log-likelihood estimates are obtained on G_2 , Figure 4 shows three sets of random generative samples from our proposed method trained with G_2 on both MNIST and OMNIGLOT, compared to real samples from the training sets. We observe the generated samples are visually consistent with the training data.

5. Conclusions

This paper presents a simple and yet effective architecture to compose normalizing flows based on 1d convolution on the input vectors. ConvFlow takes advantage of the effective computation of convolution to warp a simple density to the

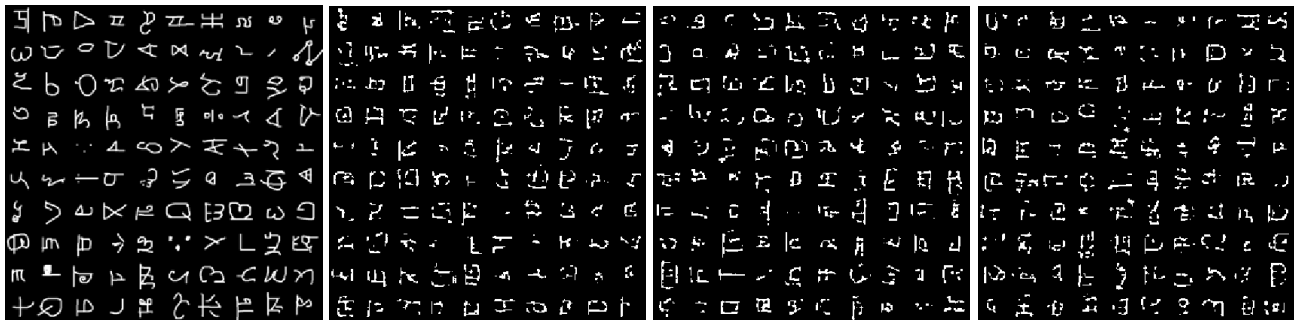
possibly complex target density, as well as maintaining as few parameters as possible. To further accommodate long range interactions among the dimensions, dilated convolution is incorporated to the framework without increasing model computational complexity. A Revert Layer is used to maximize the opportunity that all dimensions get as much warping as possible. Experimental results on inferring target complex density and density estimation on generative modeling on real world handwritten digits data demonstrates the strong performance of ConvFlow. Particularly, density estimates on MNIST show significant improvements over state-of-the-art methods, validating the power of ConvFlow in warping multivariate densities. It remains an interesting question to see how ConvFlows can be directly combined with powerful observation models such as PixelRNN to further advance generative modeling with tractable density evaluation. We hope to address these challenges in future work.

Table 2: OMNIGLOT test set NLL with generative models G_1 and G_2 (lower is better, K is number of ConvBlocks)

OMNIGLOT	$-\log p(x)$ on G_1	$-\log p(x)$ on G_2
VAE (Burda et al., 2015)	108.22	106.09
IWAE ($IW = 50$) (Burda et al., 2015)	106.08	104.14
VAE+ ($K = 1$)	108.30	106.30
VAE+ ($K = 4$)	108.31	106.48
VAE+ ($K = 8$)	108.31	106.05
VAE+IAF ($K = 1$)	107.31	105.78
VAE+IAF ($K = 2$)	106.93	105.34
VAE+IAF ($K = 4$)	106.69	105.56
VAE+IAF ($K = 8$)	106.33	105.00
VAE+ConvFlow ($K = 1$)	106.42	105.33
VAE+ConvFlow ($K = 2$)	106.08	104.85
VAE+ConvFlow ($K = 4$)	105.21	104.30
VAE+ConvFlow ($K = 8$)	104.86	103.49
IWAE+ConvFlow ($K = 8, IW = 50$)	104.21	103.02



(a) MNIST Training data

(b) Random samples 1 from IWAE-ConvFlow ($K = 8$)(c) Random samples 2 from IWAE-ConvFlow ($K = 8$)(d) Random samples 3 from IWAE-ConvFlow ($K = 8$)

(e) OMNIGLOT Training data

(f) Random samples from IWAE-ConvFlow ($K = 8$)(g) Random samples from IWAE-ConvFlow ($K = 8$)(h) Random samples from IWAE-ConvFlow ($K = 8$)

Figure 4: Training data and generated samples

References

- Blei, David M., Ng, Andrew Y., and Jordan, Michael I. Latent dirichlet allocation. *Journal of Machine Learning Research*, 3:993–1022, 2003.
- Burda, Yuri, Grosse, Roger, and Salakhutdinov, Ruslan. Importance weighted autoencoders. *arXiv preprint arXiv:1509.00519*, 2015.
- Dinh, Laurent, Krueger, David, and Bengio, Yoshua. Nice: Non-linear independent components estimation. *arXiv preprint arXiv:1410.8516*, 2014.
- Dinh, Laurent, Sohl-Dickstein, Jascha, and Bengio, Samy. Density estimation using real nvp. *arXiv preprint arXiv:1605.08803*, 2016.
- Germain, Mathieu, Gregor, Karol, Murray, Iain, and Larochelle, Hugo. Made: masked autoencoder for distribution estimation. In *Proceedings of the 32nd International Conference on Machine Learning (ICML-15)*, pp. 881–889, 2015.
- Ioffe, Sergey and Szegedy, Christian. Batch normalization: Accelerating deep network training by reducing internal covariate shift. In *Proceedings of the 32nd International Conference on Machine Learning, ICML 2015, Lille, France, 6-11 July 2015*, pp. 448–456, 2015.
- Kingma, Diederik and Ba, Jimmy. Adam: A method for stochastic optimization. *arXiv preprint arXiv:1412.6980*, 2014.
- Kingma, Diederik P and Welling, Max. Auto-encoding variational bayes. *arXiv preprint arXiv:1312.6114*, 2013.
- Kingma, Diederik P., Salimans, Tim, Józefowicz, Rafal, Chen, Xi, Sutskever, Ilya, and Welling, Max. Improving variational autoencoders with inverse autoregressive flow. In *Advances in Neural Information Processing Systems 29: Annual Conference on Neural Information Processing Systems 2016, December 5-10, 2016, Barcelona, Spain*, pp. 4736–4744, 2016.
- Lake, Brenden M., Salakhutdinov, Ruslan, and Tenenbaum, Joshua B. One-shot learning by inverting a compositional causal process. In *Advances in Neural Information Processing Systems 26: 27th Annual Conference on Neural Information Processing Systems 2013. Proceedings of a meeting held December 5-8, 2013, Lake Tahoe, Nevada, United States.*, pp. 2526–2534, 2013.
- Larochelle, Hugo and Murray, Iain. The neural autoregressive distribution estimator. In *Proceedings of the Fourteenth International Conference on Artificial Intelligence and Statistics, AISTATS 2011, Fort Lauderdale, USA, April 11-13, 2011*, pp. 29–37, 2011.
- Maaten, Laurens van der and Hinton, Geoffrey. Visualizing data using t-sne. *Journal of machine learning research*, 9 (Nov):2579–2605, 2008.
- Oord, Aaron van den, Dieleman, Sander, Zen, Heiga, Simonyan, Karen, Vinyals, Oriol, Graves, Alex, Kalchbrenner, Nal, Senior, Andrew, and Kavukcuoglu, Koray. Wavenet: A generative model for raw audio. *arXiv preprint arXiv:1609.03499*, 2016a.
- Oord, Aaron van den, Kalchbrenner, Nal, and Kavukcuoglu, Koray. Pixel recurrent neural networks. *arXiv preprint arXiv:1601.06759*, 2016b.
- Rezende, Danilo Jimenez and Mohamed, Shakir. Variational inference with normalizing flows. In *Proceedings of the 32nd International Conference on Machine Learning, ICML 2015, Lille, France, 6-11 July 2015*, pp. 1530–1538, 2015.
- Sønderby, Casper Kaae, Raiko, Tapani, Maaløe, Lars, Sønderby, Søren Kaae, and Winther, Ole. Ladder variational autoencoders. In *Annual Conference on Neural Information Processing Systems 2016, December 5-10, 2016, Barcelona, Spain*, pp. 3738–3746, 2016.
- Yu, Fisher and Koltun, Vladlen. Multi-scale context aggregation by dilated convolutions. *arXiv preprint arXiv:1511.07122*, 2015.

A. Conditions for Invertibility

The ConvFlow proposed in Section 3 is invertible, as long as every term in the main diagonal of the Jacobian specified in Eq. (10) is non-zero, i.e., for all $i = 1, 2, \dots, d$,

$$w_1 u_i h'(\text{conv}(\mathbf{z}, w)) + 1 \neq 0 \quad (21)$$

where u_i is the i -th entry of the scaling vector \mathbf{u} . When using $h(x) = \tanh(x)$, since $h'(x) = 1 - \tanh^2(x) \in [0, 1]$, a sufficient condition for invertibility is to ensure $w_1 u_i > -1$. Thus a new scaling vector \mathbf{u}' can be created from free parameter \mathbf{u} to satisfy the condition as

$$\mathbf{u}' = \begin{cases} \mathbf{u} & \text{if } w_1 = 0 \\ -\frac{1}{w_1} + \text{softplus}(\mathbf{u}) & \text{if } w_1 > 0 \\ -\frac{1}{w_1} - \text{softplus}(\mathbf{u}) & \text{if } w_1 < 0 \end{cases} \quad (22)$$

where $\text{softplus}(x) = \log(1 + \exp(x))$. The above sufficient condition works readily for other non-linearity functions h , including sigmoid, softplus, rectifier(ReLU), leaky rectifier (Leaky ReLU) and exponential linear unit (ELU), as all their gradients are bounded in $[0, 1]$.